Three-dimensional structure of ribulose-1,5-bisphosphate carboxylase/oxygenase from *Rhodospirillum rubrum* at 2.9 Å resolution

Gunter Schneider, Ylva Lindqvist, Carl-Ivar Brändén and George Lorimer[1]

Department of Molecular Biology, Swedish University of Agricultural Sciences, Uppsala Biomedical Center, Box 590, S-75124 Uppsala, Sweden and [1]Central Research and Development Department, E.I.du Pont de Nemours and Co., Wilmington, DE 19898, USA

Communicated by C.-I.Brändén

The three-dimensional structure of ribulose-1,5-bisphosphate carboxylase/oxygenase (Rubisco) from *Rhodospirillum rubrum* has been determined at 2.9 Å resolution by X-ray crystallographic methods. The MIR-electron density map was substantially improved by two-fold non-crystallographic symmetry averaging. The polypeptide chains in the dimer were traced using a graphics display system with the help of the BONES option in FRODO. The dimer has approximate dimensions of 50 × 72 × 105 Å. The enzyme subunit is a typical two-domain protein. The smaller, N-terminal domain consists of 137 amino acid residues and forms a central, mixed five-stranded β-sheet with α-helices on both sides of the sheet. The larger C-terminal domain consists of 329 amino acid residues. This domain has an eight-stranded parallel α/β barrel structure as found in triosephosphate isomerase and a number of other functionally non-related proteins. The active site in Rubisco determined by difference Fourier techniques and fitting of active site residues to the electron density map, is located at the carboxy-end of the β-strands in the α/β barrel of the C-terminal domain. There are few domain–domain interactions within the subunit. The interactions at the interface between the two subunits of the dimer are tight and extensive. There are tight contacts between the two C-terminal domains, which build up the core of the molecule. There are also interactions between the N-terminal domain of one subunit and the C-terminal domain of the second subunit, close to the active site.

Key words: Rubisco/protein crystallography/photosynthesis

Introduction

Ribulose-1,5-bisphosphate carboxylase/oxygenase (Rubisco) is the key enzyme in photosynthetic carbon dioxide fixation, responsible for the annual fixation of $\sim 10^{11}$ tons of CO_2. The enzyme catalyses the carboxylation of ribulose-1,5-bisphosphate, the initial step in the Calvin cycle. The same enzyme is also the catalyst for the first step in photorespiration, the oxygenation of ribulose-1,5-bisphosphate (Miziorko and Lorimer, 1983). This reaction substantially reduces the overall rate of photosynthesis and hence plant productivity.

Rubisco from higher plants, algae and most photosynthetic microorganisms is a multisubunit complex built up of eight large (mol. wt 56 kd) and eight small (mol. wt. 14 kd) subunits. The catalytic activities for both the carboxylation and the oxygenation reaction reside on the large subunit. The function of the small subunit is still unknown. The primary structures of the large

subunits of higher plant and algal carboxylases studied so far exhibit a high degree of amino acid homology, in the range of 70–90% (Miziorko and Lorimer, 1983).

In contrast to these carboxylases, the enzyme from the photosynthetic bacterium *Rhodospirillum rubrum* differs considerably in primary and quaternary structure. This carboxylase is only a dimer of large subunits and does not contain small subunits (Schloss *et al.*, 1979). The overall amino acid homology to the large subunit of higher plant carboxylases is 25% (Hartman *et al.*, 1982; Nargang *et al.*, 1984). Despite this low overall amino acid homology, some peptide regions are highly conserved amongst all the carboxylases. Three of these conserved regions have been identified as active site peptides (Lorimer, 1981; Herndon *et al.*, 1982; Fraij and Hartman, 1982), indicating a common active site and thus a similar three-dimensional structure for all the carboxylase large subunits.

Common to all carboxylases is an activation process, during which a lysine residue becomes carbamylated by an activator CO_2 molecule (Lorimer and Miziorko, 1980; Lorimer, 1981). The carbamate is further stabilized by a magnesium ion (Pierce and Reddy, 1986). This activation process is necessary for both the carboxylation and the oxygenation reactions. The activated ternary complex is able to react with the substrate ribulose-1,5-bisphosphate, which is subsequently attacked by either carbon dioxide or oxygen. All biochemical evidence indicates that both carboxylation and oxygenation occur at the same site in the protein (Miziorko and Lorimer, 1983).

Rubisco is the major target enzyme in attempts to improve the efficiency of photosynthesis and thus increase the productivity of agriculturally important crops. Recombinant DNA techniques seem a promising tool to modify the carboxylase/oxygenase ratio by genetic engineering. The gene from the *Rh. rubrum* carboxylase has been cloned and expressed in *Escherichia coli* (Somerville and Somerville, 1984). This gene product is a fusion peptide containing an additional 24 amino acid peptide from β-galactosidase as the N-terminus (Larimer *et al.*, 1986). However, its kinetic properties are indistinguishable from the native *Rh. rubrum* enzyme. Recently, the gene for Rubisco from *Rh. rubrum* has been cloned and expressed in *E. coli* without the 24 additional amino acids from β-galactosidase (Larimer *et al.*, 1986).

Specific mutations of Rubisco, probing the active site, have been carried out (Gutteridge *et al.*, 1984; Estelle *et al.*, 1985; Niyogi *et al.*, 1986; Terzaghi *et al.*, 1986). Detailed knowledge of the three-dimensional structure is one prerequisite for active site-directed mutagenesis, aiming at increasing the efficiency at which CO_2 competes with O_2 for the reaction. Here we report the results of the structure determination of the recombinant Rubisco from *Rh. rubrum* at 2.9 Å resolution.

Results

Electron density map

Cyclic phase refinement using the local two-fold symmetry improved the electron density map sufficiently to allow most parts
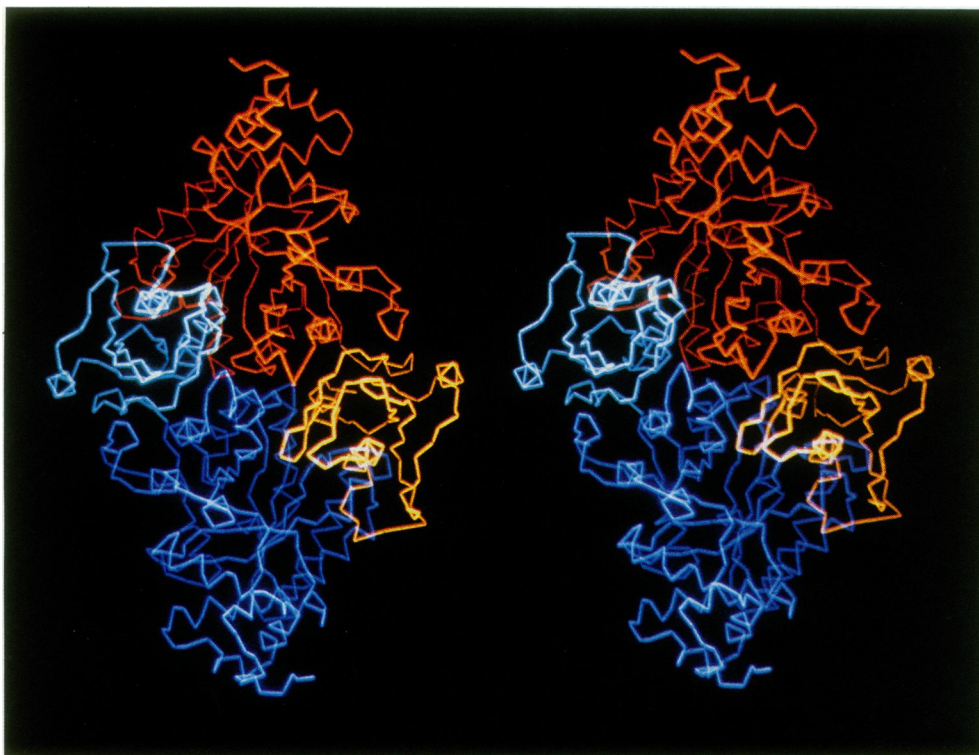
Fig. 1. Stereo view of the Cα backbone of the dimer of Rubisco. The colour scheme is as follows: Subunit 1: N-terminal domain: light blue, C-terminal domain: dark blue; Subunit 2: N-terminal domain: orange, C-terminal domain: red.
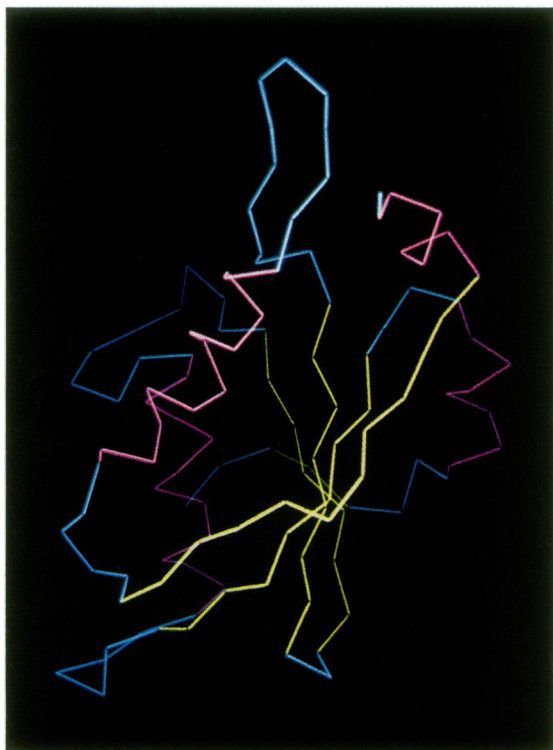

Fig. 2. Cα backbone of the N-terminal domain of one subunit of Rubisco. The strands of the mixed β-sheet are shown in yellow, the helices in pink and the connecting loops in blue.

of the chain to be traced. Our present model of Rubisco from *Rh. rubrum* includes 430 residues out of 490 amino acids. Most of the missing amino acids are at the N-terminus of the polypep-

tide chain, where there is only weak electron density for about six amino acids from Rubisco and the 24 amino acids from β-galactosidase. Furthermore, only weak density is found for ~10 residues at the C-terminal end of the polypeptide chain. There are two breaks in the electron density at two loop regions. One of these is in the N-terminal domain, where electron density for about eight amino acid residues is missing. The second break in electron density is in the loop between strand 6 and helix 6 in the C-terminal domain. In this region, there is only weak, non-continuous density for ~12 amino acid residues.

Structure of the enzyme

The dimer of Rubisco from *Rh. rubrum* has the shape of an elongated cylinder with approximate dimensions of 50 × 72 × 105 Å. Figure 1 shows the Cα-backbone for the whole dimer. The Rubisco subunit is a two-domain protein with a smaller, N-terminal domain and a larger, C-terminal domain. The core of the molecule is built up of the two C-terminal domains. There are tight and extensive interactions at the interface between the two subunits.

The N-terminal domain comprises residues 1−137. The central secondary structural motif of this domain is a five-stranded mixed β-sheet with two α-helices on one side and one α-helix on the other side of the sheet. All three helices are parallel to adjacent β-strands (Figure 2). The β-sheet is built up of βαβ, αβ and βαβ elements from the N-terminal. All the connections between the parallel strands are right handed, in agreement with other proteins whose three-dimensional structure is known (Richardson, 1976). The strand order is 5,2,4,3,1. Strands 1,2,3 are parallel to each other and strands 4 and 5 are antiparallel to these. The connection to the C-terminal domain is a short α-helix after strand 5, followed by a piece of extended chain.

The C-terminal domain consists of residues 138−466. This domain has a parallel α/β barrel structure, as found in triose-
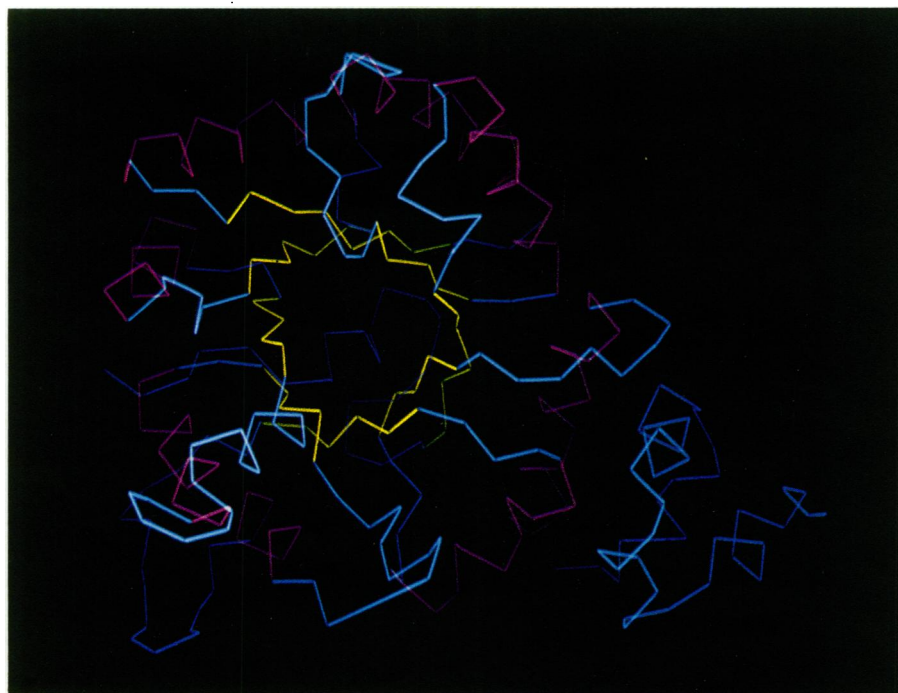
Fig. 3. Cα backbone of the C-terminal domain of one subunit of Rubisco. The eight parallel β-strands of the α/β barrel are shown in yellow, the eight helices of the barrel are shown in pink. Connecting loops and additional secondary structure elements are shown in blue.
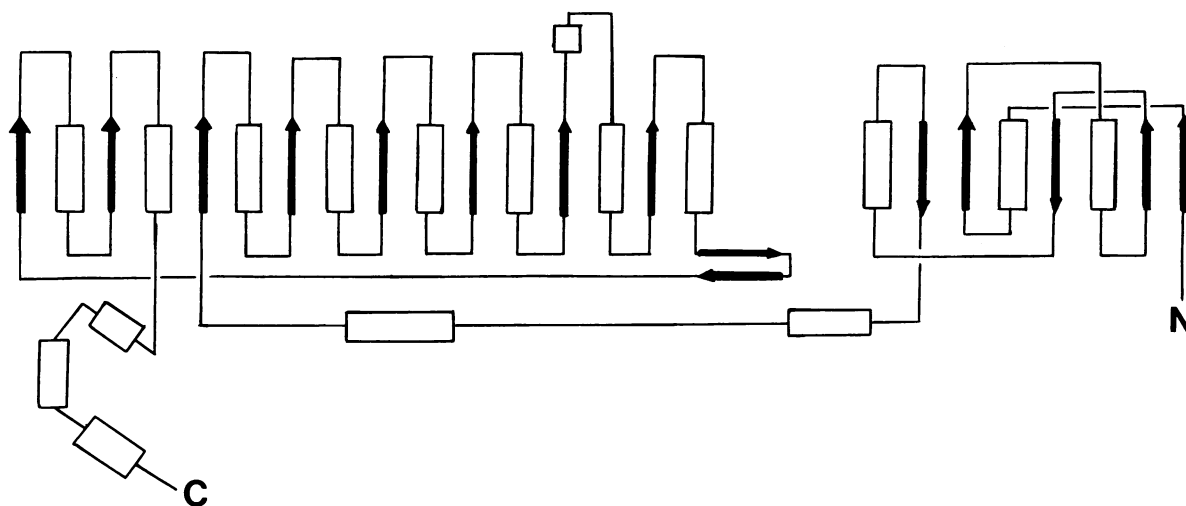

Fig. 4. Connectivity diagram for the secondary structure elements of one subunit of Rubisco. Helices are shown as rectangles and β-strands are shown as arrows.

phosphate isomerase and a number of other functionally non-related proteins. Eight parallel β-strands form the core of the barrel, which is surrounded by eight α-helices (Figure 3). The domain starts with an α-helix, at the end of the extended chain from the N-terminal domain and then the chain enters strand no. 1 of the α/β barrel. This α-helix which is not part of the barrel structure is located at the N-terminal side of the eight parallel strands — at the bottom of the α/β barrel — and thus closes off the barrel from this side. Such a helix, preceding the first strand and packed against the amino ends of the β-strands has also been observed in phospho-gluconate aldolase (Mavridis *et al.*, 1982).

There are some additional secondary structural features in this domain. An additional α-helix, not belonging to the α/β barrel motif is found after strand 5. Furthermore, after helix 6, there is a loop where the polypeptide chain forms two anti-parallel β-

strands, before the chain enters strand no. 7 of the barrel. Three more α-helices are found at the C-terminal part of the chain after helix no. 8 of the α/β barrel. Figure 4 shows a schematic connectivity diagram and Figure 5 a more topological view of the Rubisco subunit.

The active site in Rubisco could be identified both by amino acid sequence fitting to the electron density map and by difference Fourier methods. In all carboxylases, two conserved lysine residues have been shown to be close to the active site. Lys 166 has a non-specified functional role in catalysis (Herndon *et al.*, 1982; Herndon and Hartman, 1984) and Lys 191 is the site of carbamylation (Lorimer, 1981). Both residues are found in loops between the carboxy-ends of the β-strands and α-helices of the α/β barrel. Lys 166 is located in the loop after strand no. 1 and Lys 191 is the last residue of strand no. 2 of the barrel. This
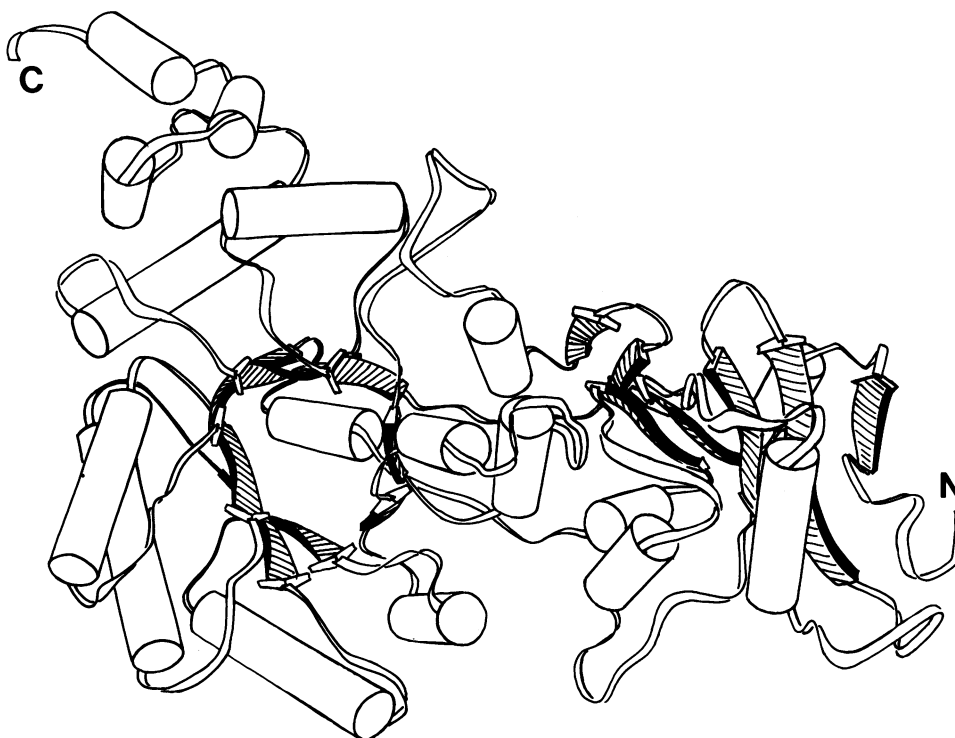
Fig. 5. Schematic diagram of the structure of one subunit of Rubisco. Cylinders represent α-helices and arrows represent β-strands. (Drawing by Ulla Uhlin.)

location of the active site in Rubisco could be confirmed by difference Fourier synthesis of modified Rubisco crystals, labelled with pyridoxal phosphate. Hartman *et al.* (1984) have shown that Lys 166 and Lys 329 are modified by this procedure. The highest peaks in the difference Fourier electron density map at 6 Å resolution were found at the carboxy-end of the β-strands of the barrel.

A comparision of the α/β barrel domain in Rubisco with glycolate oxidase, another α/β barrel protein (Lindqvist and Brändén, 1985), was carried out using the program HOMO written by M.Rossmann. The Cα-atoms of both structures were superimposed and after refinement of rotational and translational parameters and maximizing the number of overlaps, we obtained 158 equivalent Cα-atoms with a root-mean-square deviation of 2.7 Å (Figure 6). This value compares well with the values obtained from similar superpositions of other α/β barrel proteins, e.g. glycolate oxidase versus triosephosphate isomerase (Lindqvist and Brändén, 1985) and triosephosphate isomerase versus domain A of pyruvate kinase (Stuart *et al.*, 1979).

The domain–domain interactions in the Rubisco subunit are rather few. The most important involves the two anti-parallel strands after helix no. 6 of the α/β barrel. These two strands are almost parallel to the central β-sheet of the N-terminal domain close to strand 5 of this mixed sheet (Figure 5). In contrast, the subunit–subunit interactions in the dimer are tight and extensive. Two main interaction areas are found: one between the C-terminal domains of the two subunits and the second between the C-terminal domain of one subunit and the N-terminal domain of the second subunit.

Loop regions from the strands to the helices of the C-terminal domain are involved in both interaction areas. Residues from loop regions 1, 2 and 3 interact with the N-terminal domain of the second subunit. Residues from loop regions 3, 4 and 5 form homologous interactions across the local two-fold axis with cor-

responding residues of the C-terminal domain of the second subunit.

These loop regions are at the same end of the α/β barrel as the active site. For loop regions 1 and 2 the first residues of the loop contribute to the active site. Subsequent residues participate in the subunit interaction area. Both these functional aspects account for the extensive sequence homology between plant and bacterial Rubisco in these loop regions.

Discussion

The α/β barrel motif has now been observed in a number of functionally different and genetically unrelated enzymes: triose phosphate isomerase (Phillips *et al.*, 1978), pyruvate kinase (Stuart *et al.*, 1979), TAKA-amylase (Matsuura *et al.*, 1980), phosphogluconate aldolase (Mavridis *et al.*, 1982), xylose isomerase (Carrel *et al.*, 1984), and glycolate oxidase (Lindqvist and Brändén, 1985). This fold with the eight parallel β-strands forming the core of the barrel and the surrounding α-helices facing the solution seems to provide a very stable framework for a number of different biological functions. In all α/β barrel enzymes observed so far, the active site is always at the carboxy-end of the β-strands at one side of the barrel. Active site side chains come from the last residues in the β-strands or from residues in the loops between the β-strands and the α-helices. It is thus not surprising that the active site in Rubisco is found at the carboxy-end of the β-strands in the α/β barrel domain.

The three lysine residues 166, 191, 329 have been chemically identified as active site residues (Herndon *et al.*, 1982; Herndon and Hartman, 1984; Lorimer, 1981). All three are in these loop regions at the carboxy end of the β-strands; Lys 166 in loop 1, Lys 191 in loop 2 and Lys 329 in loop 6. These loop regions exhibit a much higher than average degree of sequence homology between the plant and bacterial enzymes. For loop regions 1 and 2 this high sequence homology is due not only to conservation
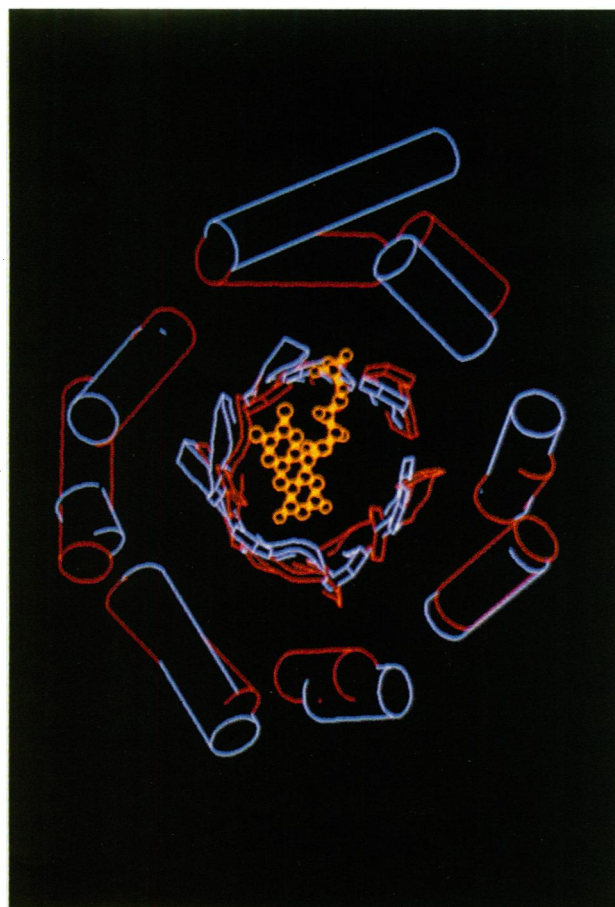
Fig. 6. Superposition of the α/β barrels of Rubisco (red) and glycolate oxidase (blue). The superposition is based on 158 equivalent atoms with an r.m.s. deviation of 2.7 Å. The cofactor FMN bound to the active site in glycolate oxidase is shown in yellow.

Table I. Data collection statistics

Compound	Number of measured reflexions	Number of unique reflexions	Resolution (Å)	R-merge[a]
Native	23 904	20 452	2.9	0.062
KAu(CN)$_2$	20 006	19 587	2.9	0.031
EMTS[b]	19 359	18 978	2.9	0.032
Sm(NO$_3$)$_3$	5716	5549	4.4	0.029
K$_2$Pt(CN)$_4$	3676	3550	5.0	0.042
Ir-cluster[c]	3950	3817	5.0	0.030
(Ethyl)$_3$PbCl	1944	1861	6.4	0.027

[a]R-merge $= \sum_h \sum_i |I(i,h) - <I(h)>| \ / \ <I(h)>$, where $I(i,h)$ is the intensity observed in the i-th source, and $<I(h)>$ is the mean intensity of the reflexion h for all measurements of $I(h)$.
[b]Ethylmercurithiosalicylate.
[c]Ir-cluster is an Iridium cluster compound (NH$_4$)$_4$[Ir$_3$N(SO)$_4$)$_6$(H$_2$O)$_3$].

of active site residues but also to participation in subunit interactions. Consequently one would expect at least part of the dimer interactions in *Rh. rubrum* Rubisco to be preserved in the octameric higher plant Rubisco.

In glycolate oxidase, the cofactor FMN binds at the same position as the substrate in triosephosphate isomerase (Lindqvist and Brändén, 1985). The phosphate binding sites for the phosphate groups of both FMN and triosephosphate are in very similar posi-

Table II. Heavy atom parameters

Derivative	Site	Occupancy[a]	Fractional coordinates			B (Å)^2
			X	Y	Z	
EMTS	1	3.2870	0.4880	0.0300	0.3030	20.9
	2	2.4184	0.7232	0.1649	0.0855	37.9
KAu(CN)$_2$	1	1.9242	0.4739	0.2966	0.2381	16.2
	2	1.6613	0.4771	0.1724	0.2123	27.4
	3	2.0649	0.6073	−0.0856	0.0886	27.9
	4	2.0391	0.5839	0.0460	0.1025	20.5
	5	1.3838	0.3932	0.0383	0.3657	33.5
	6	0.8815	0.7809	0.1714	−0.0015	30.0
Sm(NO$_3$)$_3$	1	2.4355	0.7701	0.9459	0.0900	37.2
	2	1.8610	0.5455	0.2739	0.3317	30.4
	3	1.6409	0.4807	0.7343	0.3941	44.0
	4	1.1314	0.8384	0.4611	0.0392	42.8
K$_2$Pt(CN)$_4$	1	1.9771	0.7753	0.0080	0.0075	30.0[b]
	2	2.6227	0.5205	0.1790	0.3378	30.0[b]
Ir-cluster	1	1.8670	0.7005	−0.0010	0.0455	30.0[b]
	2	1.1776	0.7003	−0.0717	0.0251	30.0[b]
	3	1.3208	0.6567	0.0333	0.0308	30.0[b]
	4	1.5774	0.5696	0.1568	0.0631	30.0[b]
	5	0.9206	0.4445	0.1823	0.3031	30.0[b]
	6	1.0728	0.4383	0.2355	0.3122	30.0[b]
	7	1.2965	0.4343	0.3028	0.3059	30.0[b]
	8	0.5730	0.4895	0.0266	0.3015	30.0[b]
	9	1.8209	0.3975	0.0591	0.2169	30.0[b]
(Ethyl)$_3$PbCl	1	2.8948	0.7623	−0.0564	0.0951	30.0[b]
	2	2.4537	0.5480	0.2842	0.3182	30.0[b]
	3	1.4562	0.7293	−0.2762	0.3411	30.0[b]
	4	0.9708	0.9055	0.4553	0.2134	30.0[b]
	5	1.0948	0.4873	−0.2674	0.3982	30.0[b]
	6	0.9453	0.8675	0.4597	0.0425	30.0[b]

[a]In arbitrary units.
[b]Not refined.

tions. In both cases, the phosphate binds at the N-terminal part of an additional α-helix, located in the loop between a β-strand and an α-helix of the α/β barrel. A similar additional α-helix is found in the present structure in loop no. 5, which very likely is one of the phosphate binding site of the substrate ribulose-1,5-bisphosphate.

As can be seen from Figure 5, no residues from the N-terminal domain can interact directly with the active site of the same subunit. In the dimer, however, parts of the N-terminal domain of one subunit are much closer to the active site in the C-terminal domain of the second subunit. The distances between the active site and this domain are too long for a direct involvement of residues from the N-terminal domain in catalysis in the conformation present in our crystals. The enzyme species in these crystals are the non-activated form of the enzyme. It is however, conceivable that conformational changes such as domain−domain rotations as a consequence of activation or substrate binding might decrease these distances. One effect of such a domain rotation would be to decrease the accessibility of the active site for solvent. The possibility of conformational changes in Rubisco during catalysis has been discussed (Bowien and Gottschalk, 1982), but not definitely answered. It should be kept in mind, however, that the non-activated form of the enzyme catalyses decarboxylation of the six-carbon reaction intermediate (Pierce *et al.*, 1986) and thus is catalytically competent.

Materials and methods

Crystallization, data collection and heavy metal derivatives

The carboxylase used in this structure determination was a recombinant Rubisco (Somerville and Somerville, 1984), containing 24 additional amino acids from
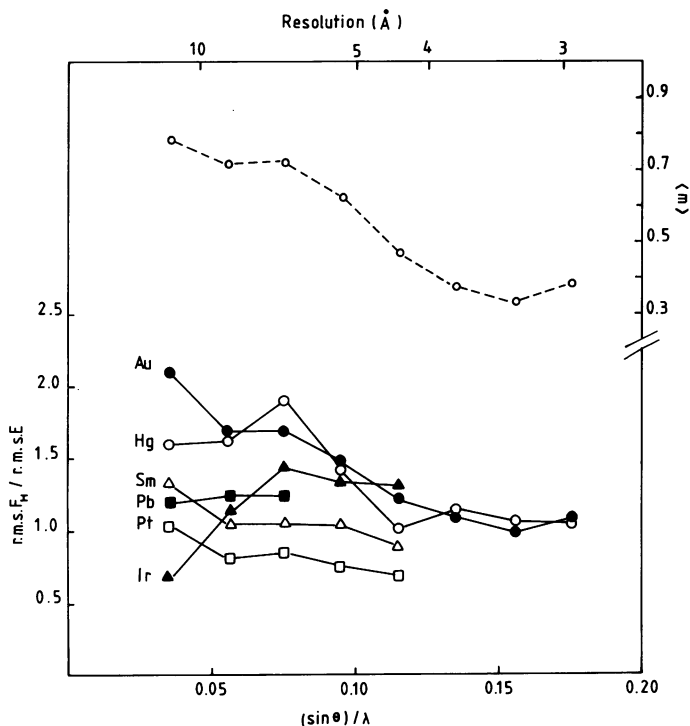
G.Schneider *et al.*

Fig. 7. Refinement statistics of the heavy-atom derivatives used for phase determination. r.m.s. F_H: root-mean square heavy atom structure factor amplitude, E: lack of closure, m: mean figure of merit.

Table III. Phase combination

Cycle	Number of atoms	R (%) 5.5–2.9 Å	Figure of merit 8.8–2.9 Å
1	–	–	0.44
2	4045	47.0	0.63
3	4288	45.7	0.64
4	4588	44.5	0.66
5	5580	42.3	0.68
6[a]	5580	38.6	0.69

Combination of partial model phases with isomorphous phases with equal weight on both contributions. The isomorphous phases were weighted by the figure of merit, the model phases according to Sim (1959) before combination.
[a]Before phase combination, the model was refined by one cycle of CORELS (Sussman *et al.*, 1977).

β-galactosidase at the N-terminus. The crystallization procedure for the non-activated enzyme has been described in detail elsewhere (Schneider *et al.*, 1986). The crystals used in this structure determination were monoclinic, spacegroup $P2_1$ with cell dimensions a = 65.5 Å, b = 70.6 Å, c = 104.1 Å and β = 92.1°. All intensity data were collected on a computer-controlled STOE single-counter four-circle diffractometer. The procedures for data collection and data processing routinely employed in our laboratory have been described in detail elsewhere (Eklund *et al.*, 1976). 24 000 reflexions for the native protein crystals were measured to give 20 500 unique reflexions to 2.9 Å resolution. Six heavy metal derivatives out of 70 tested were used for phase determination by the multiple isomorphous replacement method. Intensity data for $KAu(CN)_2$ and EMTS were collected to 2.9 Å, for $Sm(NO_3)_3$ to 4.4 Å, for $K_2Pt(CN)_4$ and an iridium cluster compound (kindly provided by R.Huber in München) to 5.0 Å and for triethyl-lead(II)chloride to 6.4 Å resolution. Details and statistics for the data collection are given in Table I. The interpretation of the difference Patterson for the EMTS derivative was straightforward in terms of two heavy atom sites per molecule. The heavy atom positions for the remaining derivatives were found by cross-difference Fourier synthesis. The heavy atom parameters were refined and the results are given in Table II and Figure 7. The overall figure of merit for all reflexions to 2.9 Å was 0.44.

As can be seen from Figure 7, the heavy atom derivatives were quite useless

for phase determination beyond 5 Å resolution. Both figure of merit and phasing power drop rapidly at higher resolution. The MIR electron density map at 2.9 Å resolution was not interpretable. B.C.Wang's solvent flattening procedure did not improve the map sufficiently to trace the polypeptide chain, probably due to the low solvent content in our crystals (~30%). However, it was rather straightforward to determine the molecular boundary for the dimer from this map except for a few contact regions at the interface between adjacent molecules.

Non-crystallographic symmetry averaging

The monoclinic crystal form used in this structure determination contains the whole dimer in the crystallographic asymmetric unit and thus has a local two-fold symmetry axis (Schneider *et al.*, 1986). The position of this axis was determined from the heavy atom sites using the HOMO program written by M.Rossmann and subsequently refined in real space using an option in the PROTEIN program system. The MIR electron density map was then symmetry averaged using G.Bricogne's non-crystallographic symmetry averaging programs (Bricogne, 1976). In a first run, all the data to 2.9 Å were included. After eight cycles of phase refinement, the R-factor had dropped from 44 to 20%. Although the averaged map had improved, it was still not possible to trace the chain. In a second run of the cyclic molecular symmetry averaging, the phase refinement was performed in steps, starting at 5 Å resolution. After convergence of refinement at 5 Å the resolution was extended in steps of one reciprocal lattice point in each direction. Available MIR phase information was included at the beginning of every resolution extension step. Seven cycles of refinement were usually sufficient to reach convergence for each step. At total of 129 cycles were run. The correlation coefficient between the observed structure factor amplitudes and the ones calculated from the averaged electron density map by Fourier inversion behaved well except at the resolution cutoffs (0.96 for all reflexions to 2.9 Å resolution). After every extension step, even the phases at lower resolution improved considerably as judged by the R factor: R = 0.44 for 5.0 Å resolution data at cycle 1, and R = 0.12 for 2.9 Å resolution data at cycle 129. Details of the structure determination will be published elsewhere.

Interpretation of the electron density map and model building

The final averaged electron density map had improved considerably. From this map, it was possible to build an initial model which contained most of the secondary structure elements and half of the connecting loops. Extensive use has been made during chain tracing and model building of the BONES option in FRODO (Jones and Thirup, 1986), a very convenient and fast way of building an initial model or rebuilding parts at a later stage.

Inclusion of partial structure information was crucial for the progress of the structure determination of Rubisco. After the initial model was built, phases were calculated from this model and combined with the MIR and averaged phases respectively. New electron density maps were calculated and the model was rebuilt. Table III shows the progress of phase combination. After five cycles of phase combination and one cycle of crystallographic refinement with CORELS (Sussman *et al.*, 1977), the R factor was 38.8%. At present, we are fitting the side chains derived from the amino acid sequence to the electron density map.

Acknowledgements

We would like to thank Dr L.Liljas for the help with the averaging program package and Mrs A.Rogelius for typing the manuscript. This work was supported by a grant from the Swedish Natural Science Research Council.

References

Bowien,B. and Gottschalk,E.-M. (1982) *J. Biol. Chem.*, **257**, 11845–11847.
Bricogne,G. (1976) *Acta Crystallogr. Sect. A*, **32**, 832–847.
Carrel,H.L., Rubin,B.H., Hurley,T.J. and Glusker,J.P. (1984) *J. Biol. Chem.*, **259**, 3230–3236.
Eklund,H., Nordström,B., Zeppezauer,E., Söderlund,G., Ohlsson,I., Boive,T., Söderberg,B.-O., Tapia,O. and Brändén,C.-I. (1976) *J. Mol. Biol.*, **102**, 27–59.
Estelle,M., Hanks,J., McIntosh,L. and Somerville,C. (1985) *J. Biol. Chem.*, **260**, 9523–9526.
Fraij,B. and Hartman,F.C. (1982) *J. Biol. Chem.*, **257**, 3501–3505.
Gutteridge,S., Sigal,I., Thomas,B., Arentzen,B., Cordova,A. and Lorimer,G. (1984) *EMBO J.*, **3**, 2737–2742.
Hartman,F.C., Stringer,C.D., Omnaas,J., Donnelly,M.I. and Fraij,B. (1982) *Arch. Biochem. Biophys.*, **219**, 422–437.
Hartman,F.C., Stringer,C.D. and Lee,E.H. (1984) *Arch. Biochem. Biophys.*, **232**, 280–295.
Herndon,C.S. and Hartman,F.C. (1984) *J. Biol. Chem.*, **259**, 3102–3110.
Herndon,C.S., Norton,I.C. and Hartman,F.C. (1982) *Biochemistry*, **21**, 1380–1385.
Jones,T.A. and Thirup,S. (1986) *EMBO J.*, **5**, 819–822.
Larimer,F.W., Machanoff,R. and Hartman,F.C. (1986) *Gene*, **41**, 75–120.

3414

Lindqvist,Y. and Bränden,C.I. (1985) *Proc. Natl. Acad. Sci. USA,* **82,** 6855–6859.

Lorimer,G.H. (1981) *Biochemistry,* **20.** 1236–1240.

Lorimer,G.H. and Miziorko,H.M. (1980) *Biochemistry,* **19,** 5321–5328.

Matsuura,Y., Kusunoki,M., Harada,W., Tanaka,N., Iga,Y., Yanaka,N., Toda,H., Narita,K. and Kakudo,M. (1980) *J. Biochem. (Tokyo),* **87,** 1555–1558.

Mavridis,I.M., Hatada,M.H., Tulinsky,A. and Lebioda,L. (1982) *J. Mol. Biol.,* **162,** 419–444.

Miziorko,H.M. and Lorimer,G. (1983) *Annu. Rev. Biochem.,* **52,** 507–535.

Nargang,F., McIntosh,L. and Somerville,C. (1984) *Mol. Gen. Genet.,* **193,** 220–224.

Niyogi,S.K., Foote,R.S., Mural,R.J., Larimer,F.W., Mitra,S., Soper,T.S., Machanoff,R. and Hartman,F.C. (1986) *J. Biol. Chem.,* **261,** 10087–10092.

Phillips,D.C., Sternberg,M.J.E., Thornton,J.M. and Wilson,I.A. (1978) *J. Mol. Biol.,* **119,** 329–351.

Pierce,J. and Reddy,G.S. (1986) *Arch. Biochem. Biophys.,* **245,** 483–493.

Pierce,J., Andrews,T.J. and Lorimer,G.H. (1986) *J. Biol. Chem.,* **261,** 10284–10256.

Richardson,J. (1976) *Proc. Natl. Acad. Sci. USA,* **73,** 2619–2623.

Schloss,J.V., Phores,E.F., Long,M.W., Norton,I.L., Stringer,C.D. and Hartman,F.C. (1979) *J. Bacteriol.,* **137,** 490–501.

Schneider,G., Bränden,C.-I. and Lorimer,G. (1986) *J. Mol. Biol.,* **187,** 141–143.

Sim,G.A. (1959) *Acta Crytallogr.,* **12,** 813–815.

Somerville,C.R. and Somerville,S. (1984) *Mol. Gen. Genet.,* **193,** 214–219.

Stuart,D.I., Levine,M., Muirhead,H. and Stammers,D.K. (1979) *J. Mol. Biol.,* **134,** 109–142.

Sussman,J.L., Holbrook,S.R., Church,G.M. and Kim,S.-H. (1977) *Acta Crystallogr. Sect. A,* **33,** 800–804.

Terzaghi,B.E., Laing,W.A., Christeller,J.T., Petersen,G.B. and Hill,D.F. (1986) *Biochem. J.,* **235,** 839–846.